Proc. Natl. Acad. Sci. USA
Vol. 89, pp. 748–752, January 1992
Biochemistry

Truncated staphylococcal nuclease is compact but disordered

(folding/polypeptide)

JOHN M. FLANAGAN*, MIKIO KATAOKA†, DAVID SHORTLE‡, AND DONALD M. ENGELMAN*

*Department of Molecular Biophysics and Biochemistry, Yale University, New Haven, CT 06511; †Physics Department, Faculty of Science, Tohoku University, Sendai, Japan; and ‡Department of Biological Chemistry, Johns Hopkins University, Baltimore, MD 21205

Communicated by Robert L. Baldwin, August 19, 1991

ABSTRACT **Deletion of 13 amino acids from the carboxyl terminus of the 149-amino acid staphylococcal nuclease molecule results in a denatured, partly unfolded molecule that lacks persistent secondary structure but is compact under physiological conditions. Since the modification is a carboxyl-terminal deletion, it is argued that the state resembles a peptide emerging from the ribosome just before the complete folding pathway is initiated. In this paper, we characterize the molecule by nuclear magnetic resonance, circular dichroism, and small-angle x-ray scattering measurements. The truncated nuclease shows wild-type levels of activity in the presence of calcium and is found to fold into a native-like conformation in the presence of 3′,5′-bisphospho-2′-deoxythymidine, a potent inhibitor. Thus, the truncated molecule retains the capacity to fold. Our results suggest that extensive solvent exclusion generates a compact polypeptide chain prior to the development of persistent secondary structural features as a protein folds during biosynthesis.**

Since the rate of protein synthesis is slow compared with the rate of folding of many small proteins from solvent-denatured states, a polypeptide emerging from a ribosome may progressively adopt conformations that precede and possibly predispose folding. Statistical mechanical analysis of a polypeptide using an average value for the bulk hydrophobicity of a protein suggests that it should be relatively compact under physiological conditions due to hydrophobic interactions (1, 2). Furthermore, while proteins may be greatly expanded under denaturing conditions (i.e., high temperature, extremes of pH, or high concentration of denaturant), they are not true random coils, since many intrachain interactions will persist. Indeed, under such conditions many proteins aggregate, showing the presence of significant interactions. Furthermore, an increasing body of data suggests that the folding process may not be entirely self-directed *in vivo*; chaperonins, proteins that bind to polypeptide chains, may play a role in some folding processes (3, 4). Because of the possible importance of knowing the state of a protein before folding to a stable structure, we have begun to characterize partly unfolded nuclease under conditions that are more nearly physiological than those previously used in studies of folding *in vitro*.

Shortle and Meeker (5) have shown that removal of the C-terminal 13 amino acids of nuclease is sufficient to destabilize the protein's native state or stabilize it in a denatured state. It was found that in nearly physiological buffers the 136-amino acid polypeptide had lost the CD spectrum of the native molecule. We have used CD, NMR, and small angle x-ray scattering (SAXS) to further define this denatured state of nuclease in solution and find that it is compact but lacks much of its native secondary structure.

The publication costs of this article were defrayed in part by page charge payment. This article must therefore be hereby marked "*advertisement*" in accordance with 18 U.S.C. §1734 solely to indicate this fact.

MATERIALS AND METHODS

Wild-type staphylococcal nuclease (Foggi strain) was overproduced and purified as described (5). Δ137–149 truncated nuclease was prepared either as described (5) or by extraction of *Escherichia coli* AR120 cells (containing the nuclease gene on a pAS1 derivative plasmid under λpL promoter control) with 6 M urea/50 mM Tris·HCl/100 mM NaCl/5 mM EDTA, pH 9.2 (4 ml/g wet weight) on ice for 20 min. Cell debris was removed by centrifugation at 30,000 rpm in a Beckman Ti45 rotor for 30 min. The supernatant was adjusted to pH 8.0 with 1 M HCl and loaded onto a 200-ml DEAE-cellulose column equilibrated with the extraction buffer (pH 8.0); the column was washed with an additional 2 vol of this buffer. The pooled DEAE flow-through and wash were loaded onto a 20-ml phosphocellulose column equilibrated in 0.3 M NH_4OAc, the column was washed with 5 vol of 0.3 M NH_4OAc, and the protein was eluted in 2 M NH_4OAc. The fractions containing nuclease were pooled and loaded on an AcA54 column equilibrated in 50 mM $(NH_4)_2CO_3$ and chromatographed in this buffer. Peak fractions from the AcA54 column, which show a single band on Coomassie-stained SDS/polyacrylamide gel, were pooled and dialyzed against 10 mM Tris·HCl/10 mM NaCl, pH 7.5, and stored at −20°C until used.

CD spectra were collected on an Aviv Associates (Lakewood, NJ) 60DS spectropolarimeter using a Hellma cuvette made of Suprasil quartz with a 0.1-mm path length. Spectra shown are the averages of seven scans. Data were collected at 0.5-nm intervals (1-s signal integration time; 1.5-nm bandwidth), corrected with the appropriate baseline scan, and smoothed using a third-order polynomial with a ±2-point averaging algorithm. In all experiments, the temperature was maintained at 20°C ± 0.2°C with a water-jacketed cuvette holder.

Purified protein for NMR experiments was dialyzed extensively against 10 mM NaCl. The samples 2.0 mM wild type (WT), 1.0 mM Δ137–149 + 2.0 mM Ca^{2+} + 1.5 mM 3′,5′-bisphospho-2′-deoxythymidine (pdTp), and 1.0 mM Δ137–149 (0.5 ml each) were lyophilized twice from 0.5 ml of 99.9% ^2H_2O and resuspended in 0.5 ml of ^2H_2O. WT nuclease was then incubated at 40°C for 10 min to exchange residual amides, and all three samples were lyophilized again and resuspended in 0.5 ml of 99.999% ^2H_2O. The apparent pH was adjusted to 7.5 with 1 M NaO^2H. ^1H NMR spectra in ^2H_2O were obtained at 24°C in a Bruker AM500 NMR spectrometer over a spectral width of 5000 Hz into 16,000 data points. The small residual water signal was suppressed by low-power irradiation during the relaxation delay of 2 s.

For solution scattering, concentrated stock solutions (10–15 mg/ml) of WT and Δ137–149 nuclease samples were dialyzed at room temperature against 10 mM NaCl/10 mM Tes, pH 7.5, overnight. For samples containing ligands, Ca^{2+} was added in a 2.2-fold molar excess, and pdTp was added in

Abbreviations: SAXS, small-angle x-ray scattering; pdTp, 3′,5′-bisphospho-2′-deoxythymidine; WT, wild type.

a 1.2-fold molar excess just prior to data acquisition. SAXS data were collected at the Photon Factory in Japan (6) or at Yale University on a small-angle scattering station as described (7). The correction for the protein concentration dependence of the scattered intensity to obtain the scattering curves at infinite dilution has been described (7). In all cases, the buffers used in the subtraction were the final dialyzate with the addition of appropriate solutes where needed.

RESULTS AND DISCUSSION

Fig. 1 shows the CD spectra of truncated nuclease Δ137–149 and of WT native nuclease. The WT CD spectrum is that of an $\alpha + \beta$ protein, as is expected from the crystal structure (8, 9). However, the CD spectrum of Δ137–149 differs significantly from that of folded nuclease and shows that roughly half of its helical secondary structure has been lost, as indicated by the molar ellipticity at 222 nm. These results are in agreement with previous work (5). Attempts to fit the CD spectrum of Δ137–149 with combinations of spectra for α-helix, β-sheet, and coil have been unsuccessful. This result would not be surprising for a substantially denatured molecule, since unstructured or random configurations are not well represented in sets of commonly used basis spectra (10, 11).

An important feature of Δ137–149 is that it is competent to adopt a folded conformation. Shortle and Meeker (5) found that the truncated polypeptide is fully active at low salt concentrations on a DNA substrate. Furthermore, addition of pdTp, a competitive inhibitor of nuclease, in the presence of Ca^{2+} drives the conformation of the polypeptide to the folded state, as shown in Fig. 1*B*. Both pdTp and DNA bind very tightly to the native state of nuclease, with a dissociation constant for pdTp of $\approx 1.5 \times 10^{-8}$ M (30); thus, the binding

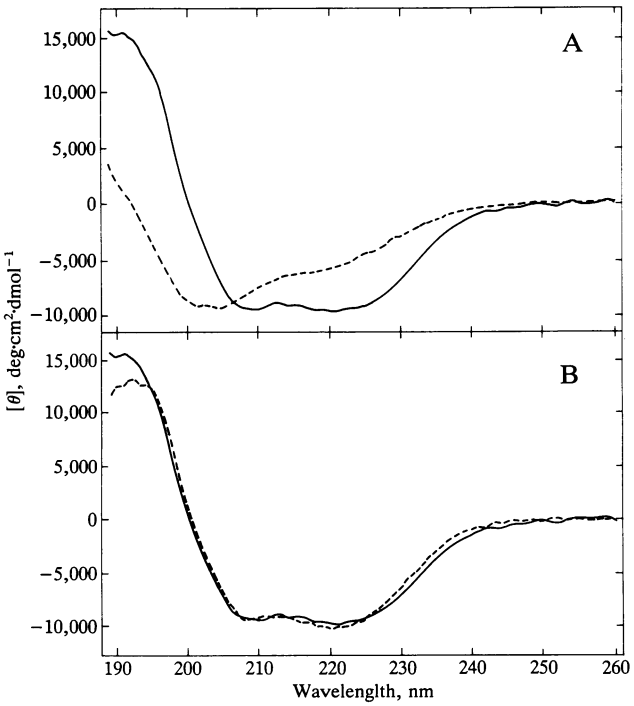

FIG. 1. CD spectra of staphylococcal nuclease. (*A*) Wild type (——) and Δ137–149 truncated (– – –) nuclease polypeptide chains (1 mg/ml) and 10 mM TES (pH 7.5). (*B*) Wild-type (——) and Δ137–149 with 10 mM $CaCl_2$ and 70 μM pdTp (– – –). Purified protein was dialyzed exhaustively against 10 mM TES (pH 7.5) (*A* and *B*) and in the case of the Δ137–149 spectrum in *B*, pdTp and $CaCl_2$ were added from concentrated stock solutions just prior to acquisition of the spectra. Note the loss of secondary structure upon deletion of the 13 C-terminal amino acids and its restoration upon binding pdTp.

of pdTp to the folded state will increase its relative stability compared to the denatured state, to which it is expected to bind much more weakly. Assuming no binding to the denatured states, the apparent binding constant of pdTp to Δ137–149 was found to be significantly weaker than to WT, and the difference in the apparent binding constants was used to calculate an equilibrium constant between the folded and denatured states of Δ137–149 of ≈160 (5). We have examined the interaction of pdTp with WT and Δ137–149 by titration calorimetry and found not only that the apparent binding constant of pdTp is smaller for Δ137–149, but also that the enthalpy ΔH of binding is significantly larger for this truncated protein than for WT (J.M.F., L. Goshianni, D.M.E., and J. Sturtevant, unpublished data). This is consistent with the idea that pdTp binding drives Δ137–149 to the native state, the increase in ΔH of binding being related to the enthalpy of folding.

The ^1H NMR spectra in ^2H_2O of folded WT, and Δ137–149 with and without pdTp are shown in Fig. 2. In each case, the amide protons were fully exchanged with deuterons. The complete exchange of amide protons of WT requires incubation of the protein sample in ^2H_2O at 40°C for 10 min (12), while for Δ137–149 no heating is required. Spectra obtained in H_2O show no extremely stable amides in Δ137–149, although there appear to be a few protected on the 100-ms time scale at pH 7.5. The instability of the amide protons shows that there is little stable structure in Δ137–149 and that whatever amount is present is much more solvent accessible than in WT. Thus, the remaining secondary structure seen by CD is transient.

The chemical shift dispersion seen in the NMR spectrum of Δ137–149 is significantly less than that observed for WT. It is, however, not that of a random collection of amino acids. This can be seen in the C_α region where a few C_α protons are found downfield of the residual $^1H^2HO$ peak. In addition, there appear to be several ring current-shifted methyl groups near 0.2 ppm that disappear upon heating (data not shown). Importantly, there is little chemical-shift dispersion seen for the four C-4 histidine ring protons. We find only one peak whose integrated intensity represents four protons resonating at 7.87 ppm. These histidine C-4 resonances have been used in several previous studies as reporters of structural heterogeneities in the native and thermally denatured states of nuclease (12, 13). The lack of dispersion for these residues in Δ137–149 is surprising in light of the chemical shift dispersion in other regions of the spectrum. It is unlikely that the four histidines at positions 8, 46, 121, and 124 are involved in residual stable structure in Δ137–149.

As expected from the changes seen using CD, addition of pdTp and Ca^{2+} produces large changes in the NMR spectrum of Δ137–149 (Fig. 2). Qualitatively, pdTp and Ca^{2+} greatly increase the dispersion of the spectrum. In particular, the single resonance at 7.87 ppm in the unliganded spectrum, corresponding to the four histidine C-4 protons, is split into four separate resonances in the region between 7.6 and 8.0 ppm in the presence of pdTp and Ca^{2+}. In addition, the number of downfield-shifted C_α protons between 5.0 and 6.0 ppm, and the upfield ring current-shifted methyl protons between 1.2 and 0.0 ppm in the liganded protein are now similar to those observed in WT (Fig. 2).

Addition of pdTp in substoichiometric quantities produces a spectrum consisting of resonances corresponding to both folded and denatured states (data not shown), showing that the folded and denatured states are in slow exchange on the proton NMR time scale. We have also observed that addition of pdTp and Ca^{2+} increases manyfold the number of solvent-protected amides with lifetimes of at least 100 ms (data not shown). These observations support our view that pdTp and Ca^{2+} stabilize the folded state of Δ137–149.

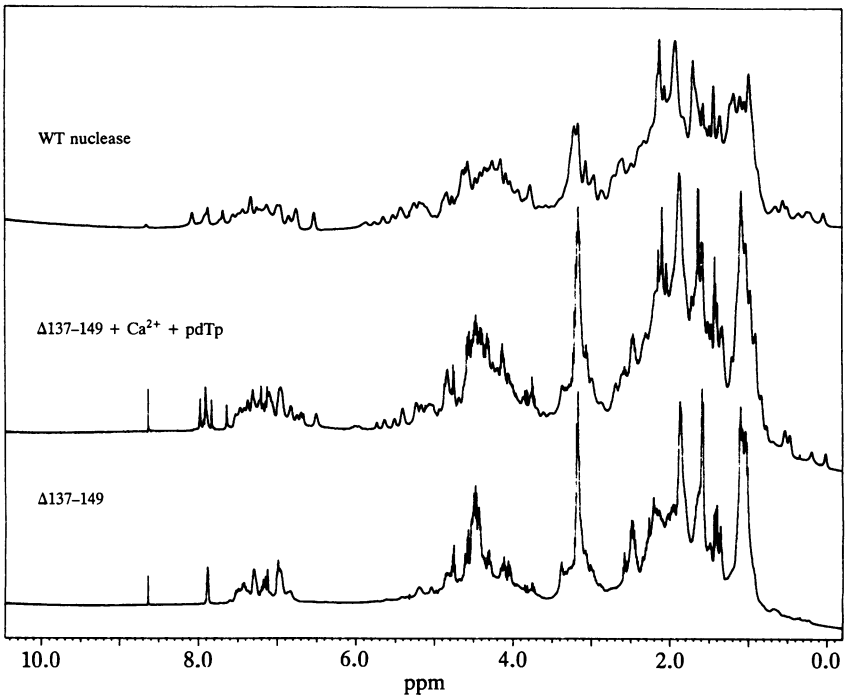

FIG. 2. ^1H NMR spectra of staphylococcal nuclease in ^2H_2O. Top trace, WT; middle trace, Δ137–149 with pdTp and Ca^{2+}; bottom trace, Δ137–149 in the absence of ligand. Deletion of the 13 C-terminal amino acids results in a loss of histidine chemical shift dispersion and a reduction of ring current-shifted methyl and downfield-shifted C_α protons. Binding of pdTp reverses these effects.

Both CD and NMR are sensitive to local environments in the polypeptide—CD primarily to helical secondary structure and NMR both to secondary structure and to local packing or electrostatic environments. Neither is particularly sensitive to the overall arrangement of the polypeptide chain. Therefore, we have used SAXS to probe the overall conformation of Δ137–149 by measuring its radius of gyration, which is extremely sensitive to the spatial extent of the particle since it is the second moment of the electron distribution. For any particle, there is a region near the direction of the incident beam where the scattered intensity (I) as a function of angle (2θ) is approximately gaussian (ref. 14 and references therein). In this "Guinier" region a plot of ln $I(Q)$ vs. Q^2 [$Q = (4\pi \sin\theta)/\lambda$; λ = radiation wavelength] will be linear and the slope will be related to the electronic radius of gyration (R_g)

$$R_g^2 = \frac{\sum_i \rho_i r_i^2}{\sum_i \rho_i},$$

where ρ_i = electron density and r_i = distance from center of mass. In addition, in a SAXS experiment, one can determine the volume of a particle from the extrapolated intensity at zero angle [$I(0)$], from which the molecular weight can be derived if the concentration and partial specific volume of the scattering molecule are known. If the molecular weight is known, as in the present case, $I(0)$ provides a test for aggregation.

Comparisons of the Guinier regions of WT, Δ137–149, and Δ137–149 with pdTp and Ca^{2+} are shown in Fig. 3. The R_g determined from this region for WT is 16.2 Å, while that of the Δ137–149 truncated polypeptide is 21.2 Å (Fig. 3*A*). Addition of pdTp and Ca^{2+} to Δ137–149 decreases R_g to 15.8 Å (Fig. 3*B*). The relatively small value of R_g of unliganded Δ137–149 may be compared with the R_g of WT nuclease in 5 M urea of nearly 35 Å (data not shown), or with the R_g expected for a random 136-amino acid polypeptide of >40 Å (15). Thus, Δ137–149 nuclease adopts a compact though nonnative conformation under nearly physiological conditions.

A major concern in studies of denatured polypeptides is whether aggregation has occurred. The linearity and weak concentration dependence of the Guinier plots encourage the view that aggregation is minimal. Most importantly, the $I(0)$ measurements give the molecular weight value expected for monomers.

An alternative interpretation of our results might be that truncation of the 13 C-terminal residues only destabilizes the

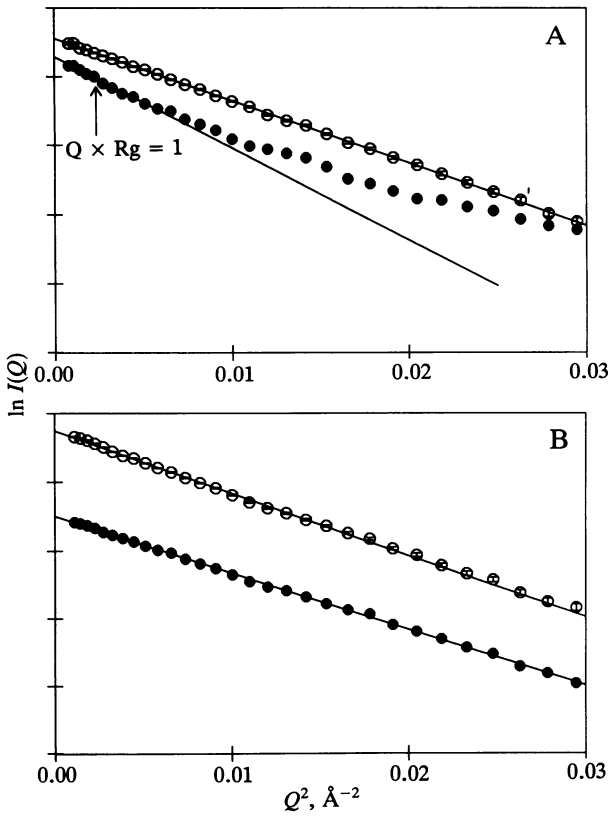

FIG. 3. Comparison of SAXS curves of nuclease at infinite dilution. (*A*) Guinier plot of Δ137–149 with (●) and without (○) pdTp and Ca^{2+}. (*B*) Guinier plot of nuclease (○), and Δ137–149 truncated nuclease (●). Curves are separated for clarity. Note that different regions of Q^2 are shown in *A* and *B*. Truncation of the nuclease increases the slope somewhat; addition of pdTp reverses the change.

protein moderately, such that at 25°C 20–40% of the molecules are folded (compact) and the remainder are denatured (expanded). This view seems incorrect since the R_g of Δ137–149 is nearly independent of temperature (5°C–30°C) and pH (pH 8–4), whereas the equilibrium between the folded and denatured conformations should be altered by variations of temperature and pH. In addition, such an explanation seems inconsistent with our proton NMR data since it would mean that the folded and denatured conformations must be in fast exchange. From the observed proton resonances of the histidines, the folding/unfolding rates would have to be <1 ms, which is in conflict with observed folding rates for WT nuclease of 2–4 s (13). Furthermore, studies of pdTp and Ca^{2+} binding by Δ137–149 show that >99% of the unliganded molecules are nonnative (5).

Additional scattering curves collected to larger angles give information regarding the overall structure of the particle, including its longest dimension (ref. 14 and references therein). A real-space representation of the information in the scattering curve can be obtained by using a Fourier inversion of scattered intensity to derive a radial Patterson [P(*r*)] curve. The information in this representation is the length distribution of atom-weighted interatomic vectors in the particle. Fig. 4 shows P(*r*) curves for WT, and Δ137–149 with and without Ca^{2+} and pdTp calculated from the scattering data using the algorithm of Moore (16). The P(*r*) curve of WT folded nuclease is characteristic of a roughly spherical particle having a longest chord of 47 Å and closely matches the P(*r*) curve computed from the nuclease crystal coordinates (data not shown). The P(*r*) curve of Δ137–149 in the presence of pdTp and Ca^{2+} is nearly identical to that of folded nuclease. In contrast, the P(*r*) curve of Δ137–149 in the absence of ligands is strikingly different from that of WT or Δ137–149 + pdTp and Ca^{2+}. The longest chord in the molecule appears to be ≈63 Å, and the particle can no longer be best described as spherical but is instead more elongated. Table 1 summarizes the various parameters obtained from the Guinier and P(*r*) analyses.

A unique interpretation of P(*r*) curves is impossible due to the loss of orientational information inherent in the solution experiment. However, a shape that is compatible with the data is a dumbbell structure, similar to that observed in calmodulin (7, 17, 18). In fact, the P(*r*) curves of calmodulin and Δ137–149 are remarkably similar [see P(*r*) curves (7)], but

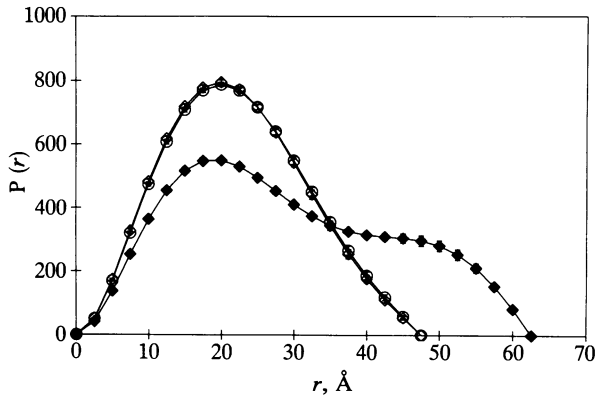

FIG. 4. Radial distance distribution function P(*r*) from solution x-ray scattering data for nuclease. Curves are shown for WT (○) and Δ137–149 with (◇) and without (◆) pdTp and Ca^{2+}. P(*r*) curves were calculated by the method of Moore (16) from data extrapolated to infinite dilution. The angular range used in the data processing typically begins at the minimum Q used in Guinier analysis and ends at a Q_{max} of $Q \cdot R_g = 5$. For these curves, the minimum Q corresponds to 1/300 Å; however, inclusion of data to 1/800 Å has little effect on the P(*r*) curves. Smearing of the scattered intensity due to beam geometry was eliminated by the method in ref. 16.

Table 1. Summary of parameters from SAXS experiments

	Smeared R_g (Guinier), Å	Desmeared R_g (Moore), Å	d_{max}, Å
WT nuclease	15.9 ± 0.2	16.2 ± 0.2	47.0 ± 2
Δ137–149	20.2 ± 0.4	21.2 ± 0.2	63.0 ± 2
Δ137–149 + pdTp + Ca^{2+}	15.6 ± 0.2	15.8 ± 0.2	47.0 ± 2

d_{max}, Longest chord in the molelcule.

detailed examination of the dependence of scattered intensity as a function of angle suggests that the similarity is not complete (data not shown). The differences may arise from the partial coil character of Δ137–149, while calmodulin is purely globular. A detailed discussion of the extended scattering curves of Δ137–149 will be presented elsewhere. A second possible model that could explain the scattering data for Δ137–149 is a relatively compact core with a disorganized tail(s). The tail(s) might be composed primarily of charged residues, while the core might be formed by removal of many of the hydrophobic residues from full contact with solvent. This second model is not completely inconsistent with the two-domain, or dumbbell, model; one might postulate that there is a compact domain and a second disorganized domain. Of course, there are a large number of models that could, in principle, explain the scattering curves. These two models are interesting in that they are physically plausible and can be tested by further studies.

Anfinsen (19) originally proposed that nuclease folding might be organized around two folding centers, one lying in the N-terminal half and the other in the C-terminal portion. He argued that these regions fold independently, subsequently interacting to give the final folded conformation. Our results are consistent with the general character of this model except that it is unlikely that these denatured domains adopt a near-native structure, since stable secondary structure is largely absent.

Our data provide support for several interesting speculations concerning the folding process. That the Δ137–149 truncated polypeptide exists in an extremely compact state having only transient secondary structure is consistent with the idea that a hydrophobic core forms as a polypeptide emerges from a ribosome and that stable secondary structure is formed later. In contrast, several NMR studies appear to support the framework model for protein folding (20, 21), but the difference may be easily understood in that the hydrophobic core suggested by our data would not give rise to a significant number of protected amides. A recent study of barnase, RNase from *Bacillus amyloliquefaciens*, suggests that a compact core forms early in the folding process (22), which would be consistent with our nuclease results.

But how can a hydrophobic core form in the absence of stable secondary structure when water must be expelled, presenting a problem in satisfying backbone hydrogen bond requirements? In either of our models for the structure of Δ137–149, we see that the protein conformation is elongated. In fact, in one model there are two relatively independent domains, creating a high surface/volume ratio and permitting many solvent contacts while still burying hydrophobic residues. This means that many amides could still be in contact with solvent. Transient hydrogen bonding and the participation of small numbers of water molecules could also permit a compact, disordered core to exist while excluding bulk water. The residual secondary structure shown by CD could contribute some transient hydrogen bonding.

The synthesis of proteins on the ribosome is orders of magnitude slower (23) than the rate of folding of many small proteins studied *in vitro*. The conformation of the first 136 residues of nuclease may be similar to the polypeptide chain just prior to the completion of its synthesis and release from

a ribosome, and our data show that a significant degree of compaction of the chain would occur cotranslationally as suggested by several authors (24, 25).

Our results strongly support the idea that the denatured state of a long polypeptide under physiological conditions is not a random coil and that the polypeptide chain is condensed. While some secondary structure is present, it is not necessarily related to secondary structures found in the folded protein, and it is clearly unstable. This is in contrast to the compact denatured state termed the molten globule, which is seen in some proteins at low pH and high salt (26, 27) and which is thought to contain most of the secondary structure with few persistent tertiary interactions (27, 28). For α-lactalbumin, this state is as compact as the native and appears to have a similar packing of secondary structure to that of folded α-lactalbumin (26, 29). The state we describe in the case of truncated nuclease does not appear to correspond to the molten globule state as described for α-lactalbumin. The folding of truncated nuclease promoted by pdTp and Ca^{2+} occurs with a large increase in stable secondary structure and a relatively small change in overall size.

We are indebted to Drs. Thomas Jue and Christopher Dempsey for their help with collecting the ^1H NMR spectra. We would like to acknowledge support from the National Institutes of Health. M.K. is grateful to the Ministry of Education, Culture and Science of Japan, and to the Photon Factory.

1. Dill, K. A. (1985) *Biochemistry* **24,** 1501–1509.
2. Dill, K. A. (1990) *Biochemistry* **31,** 7133–7155.
3. Rothman, J. E. (1989) *Cell* **59,** 591–601.
4. Osterman, J., Horwich, A. L., Neupert, W. & Hartl, F. (1989) *Nature (London)* **341,** 125–130.
5. Shortle, D. & Meeker, A. K. (1989) *Biochemistry* **28,** 936–944.
6. Ueki, T., Hiragi, Y., Kataoka, M., Inoko, Y., Amemiya, Y., Izumi, Y., Tagawa, H. & Muroga, Y. (1985) *Biophys. Chem.* **23,** 115–124.
7. Kataoka, M., Head, J. F., Seaton, B. A. & Engelman, D. M. (1989) *Proc. Natl. Acad. Sci. USA* **86,** 6944–6948.
8. Cotton, F. A., Hazen, E. E. & Legg, M. S. (1979) *Proc. Natl. Acad. Sci. USA* **76,** 2551–2555.
9. Loll, P. J. & Lattman, E. E. (1989) *Proteins Struct. Funct. Genet.* **5,** 183–201.
10. Yang, J. T., Wu, C.-S. C. & Martinez, H. M. (1986) *Methods Enzymol.* **130,** 208–269.
11. Compton, L. A. & Johnson, W. C. (1986) *Anal. Biochem.* **155,** 155–187.
12. Alexandrescu, A. T., Hinck, P. A. & Markley, J. L. (1990) *Biochemistry* **29,** 4516–4525.
13. Evans, P. A., Kautz, R. A., Fox, R. O. & Dobson, C. M. (1989) *Biochemistry* **28,** 362–370.
14. Glatter, O. & Kratky, O., eds. (1986) *Small Angle X-ray Scattering* (Academic, London).
15. Tanford, C., Kawahara, K. & Lapanje, S. (1966) *J. Biol. Chem.* **241,** 1921–1923.
16. Moore, P. B. (1980) *J. Appl. Crystallogr.* **13,** 168–175.
17. Seaton, B. A., Head, J. F., Engelman, D. M. & Richards, F. M. (1985) *Biochemistry* **24,** 6740–6743.
18. Heidorn, D. B. & Trewhella, J. (1988) *Biochemistry* **27,** 909–915.
19. Anfinsen, C. B. (1972) *Biochem. J.* **128,** 737–749.
20. Roder, H., Elove, G. A. & Englander, S. W. (1988) *Nature (London)* **335,** 700–704.
21. Udgaonhar, J. B. & Baldwin, R. L. (1988) *Nature (London)* **335,** 694–699.
22. Matouschek, A., Kellis, J. T., Serrano, L., Bycroft, M. & Fersht, A. R. (1990) *Nature (London)* **346,** 440–445.
23. Peters, T., Jr., & Davidson, K. (1982) *J. Biol. Chem.* **257,** 8847–8853.
24. Bergman, L. W. & Kuehl, W. M. (1979) *J. Biol. Chem.* **254,** 8869–8876.
25. Purvis, I. J., Bettany, A. J., Santiago, T. C., Coggins, J. R., Duncan, K., Eason, R. & Brown, A. J. (1987) *J. Mol. Biol.* **193,** 413–417.
26. Dolgikh, D. A., Gilmanshin, R. I., Brazhnikov, E. V., Bychkova, V. E., Semisotnov, G. V., Venyaminov, S. Y. & Ptitsyn, B. (1981) *FEBS Lett.* **136,** 311–315.
27. Jeng, M.-F., Englander, W. S., Elove, A. G., Wand, A. S. & Roder, H. (1990) *Biochemistry* **29,** 10433–10437.
28. Baum, J., Dobson, C. M., Evans, P. A. & Henly, C. (1989) *Biochemistry* **28,** 7–13.
29. Dolgikh, D. H., Abaturov, L. V., Bolotina, I. A., Brazhnikov, E. V., Bychkova, V. E., Gilmanshin, R. I., Lebedev, Y. O., Semisotnov, G. V., Tiktopulo, E. I. & Ptitsyn, O. B. (1985) *Eur. Biophys. J.* **13,** 109–121.
30. Serpersu, E. H., Shortle, D. & Mildvan, A. S. (1986) *Biochemistry* **25,** 68–77.